

Effect of ZnS as an Impurity on the Physical Properties of KDP Single Crystals

O. V. Mary Sheeja, C. K. Mahadevan

Physics Research Centre, S.T. Hindu College, Nagercoil-629002, India,

ABSTRACT

Pure and ZnS doped KDP (KH_2PO_4) single crystals were grown from aqueous solutions by the slow evaporation technique at room temperature. The influence of ZnS on the growth and characteristic properties of the KDP single crystals were examined. Powder X-ray diffraction, atomic absorption spectroscopic and Fourier transform infrared spectral measurements were done to characterize the grown crystals structurally and chemically. Thermal and mechanical stabilities were understood by making respectively the thermogravimetric and microhardness measurements. The optical transparency and second harmonic generation efficiency were understood by making respectively the UV-Vis-NIR spectral and nonlinear optical measurements. The AC and DC electrical measurements made on all the six grown crystals indicate a normal dielectric behaviour. The electrical parameters, viz. dielectric constant, dielectric loss factor, AC electrical conductivity and DC electrical conductivity are found to increase with the increase in temperature in the temperature range (40 – 150°C) considered in the present study. The AC and DC activation energies estimated are found to vary nonlinearly with the impurity concentration.

Keywords - Crystal growth, Doped crystals, KDP crystals, Physical Properties, X-ray diffraction

I. INTRODUCTION

Single crystals of potassium dihydrogen phosphate (KDP) draw the special attention due to their unique collection of properties: the wide range of transparency, electrooptical and piezooptical effects, relatively high value of second-order nonlinear susceptibility and the possibility of growing the large-size crystals. The electrooptical property of KDP leads to the application such as polarization filter, electronic light shutter, optical rectifier, electronic light modulator, piezo optic resonator, transducer, etc. KDP belongs to scalenohedral (12 sided polyhedron) class of tetragonal crystal system having tetramolecular unit cell having $\bar{1}42d$ space group with lattice parameters: $a=b=7.448 \text{ \AA}$ and $c=6.977 \text{ \AA}$ [1,2]. It is also ferroelectric, well below room temperature, i.e below at its Curie temperature $T_c=123\text{K}$ [3,4]. Since KDP group crystal contain a large number of hydrogen bond, they can effectively capture impurity centers of a different nature. This favours their use as model object in search of new memory element, nonlinear optical and active laser media [5,6]. Many researchers have tried to modify the properties and growth rate of KDP crystal either changing the growth conditions or by adding suitable impurities [7-18]. The NLO and other properties of the crystal have been improved by doping organic and inorganic impurities [7-18].

A promising trend in the development of up-to-date functional optical materials based on dielectric is incorporation of nanoparticles into the crystalline

matrices of traditional nonlinear optical materials, for the improvement of the efficiency of their nonlinear optical response. For instance, in [19] an attempt was made to design a composite optical material possessing the properties of active laser and nonlinear optical media, the combination “KDP crystal-SiO₂ particles” being used as a model system. The influence of the size of the particles on the probability of their capture was studied, and the growing crystal was shown to be able to capture effectively 1×10^{-2} -250 μm SiO₂ particles. Recently, the effect of titanium dioxide nanoparticles on the functional properties of KDP single crystals was studied [20-24]. It was reported that the incorporation of titanium dioxide nanoparticles into KDP matrix was shown to be the composite system KDP:TiO₂ having giant nonlinear optical response. The influence of incorporated Al₂O₃.nH₂O nanoparticles on the growth kinetics of KDP crystal faces and crystal perfection were also investigated [25].

Nowadays nanocrystals are having an increasing importance due to their influence in the mechanical, electrical, optic and magnetic properties due to the quantum confinement stimulated by size decreasing. The incorporation of organic dye molecules or nanoparticles subsystems in the crystal lattice of the KDP type nonlinear optical (NLO) material is the promising approach to the controlled efficiency enhancement of their NLO response [20]. The synthesis and properties of highly luminescent II-VI compound semiconductor nanoparticles have been

extensively investigated from the basic research point of view to the application field. With the miniaturization of the particles the band gap expands and the energy level of the core band shift towards higher binding energy, and, subsequently, some physical properties change. Electron and phonon confinement is possible by II-VI compound semiconductor when size of particles become less than the Bohr radius of the bulk crystal exciton. This leads to new physical properties and, consequently, new applications arises in telecommunications and transmission [26].

Recently, a strong interest has been devoted to nanocrystals (NCs) of semiconductors embedded in wide gap matrix such as glass [27-29]. Some reports show the details of nanocrystals embedded in alkali halides crystalline lattices. Researchers have successfully embedded ZnO nanocrystals in KBr crystal [30]. Boudine et al. [31-33] have analysed alkali halides NaCl, KCl, KBr doped with II-VI compound semiconductors CdTe, CdS. A study was performed to prove the possibility of embedding II-VI compound CdTe nanoparticle in KDP crystalline matrix [34]. Such crystals are able to capture 2nm-250 μ m particles. Balasubramanian et al [35] have found that the density and mechanical properties of TGS crystals were improved by doping water soluble CdS nanoparticle dispersed in water.

Zns is an important semiconductor material with large band gap (~3.6 eV) at room temperature [36], high refractive index (2.35 at 632nm), high effective dielectric constant (9 at 1MHz) and wide wavelength passband (0.4-13 μ m). Its optical properties make it useful as a filter, reflector and planar wave guide [37]. It has a vast potential for use in optoelectronics and in electroluminescent devices [38]. Generally II-VI compound including ZnS do not dissolve in water. Now, the challenging question is how to find the way to dissolve ZnS in the aqueous solution of KDP used for the growth of single crystals. So finding a simple synthetic method to prepare ZnS is one of the main challenges of recent research activities. The aggregation of nanocrystals always decreases their nanoeffects. During the wet chemical synthesis of nanoparticles, organic stabilizers are usually used to prevent them from aggregating by capping their surface. Moreover, the introduction of stabilizers also influences on the chemical properties as well as to the physical properties of semiconductor materials, from stability to solubility and to light emission. Therefore, proper surface modification by stabilizer can remove the localized surface trap states and significantly increases the quantum yield of the excitonic emission. However, only few reports describe the preparation of water-soluble CdS nanoparticles with complex molecules used as stabilizer and capping agent

[39,40]. Recently Tang et al [41] reported that ethylene diamine capped CdS nanoparticles enhances the solubility of CdS nanoparticles in water.

In the present study, we have made an attempt to introduce ZnS as dopant into the KDP crystal matrix. We have prepared ZnS nanoparticles by using ethylene diamine as a capping agent by a simple solvothermal method using a domestic microwave oven (Mahadevan's method [42-44]). Pure and ZnS doped KDP single crystals (a total of six) were grown and characterized chemically, structurally, thermally, mechanically, optically and electrically by using the available standard methods. The results obtained are reported herein and discussed.

II. EXPERIMENTAL DETAILS

2.1 Preparation of ZnS nanoparticles

Mahadevan's method [42-44] was adopted to obtain ethylene diamine capped ZnS nanoparticles from zinc acetate dihydrate and thiourea (both AR grade) dissolved in double distilled water in the presence of ethylene diamine. The solubility was found to be 0.71g/100ml of H₂O. Details on the preparation and characterization of ZnS nanoparticles appear elsewhere.

2.2 Growth of single crystals

Pure and ZnS doped KDP single crystals were grown by the free (slow) evaporation method from saturated aqueous solutions of KDP. ZnS nanoparticles (0.1g) were dissolved in double distilled water (100ml) and used as the dopant. Five different dopant concentrations were considered by adding 2,3,4,5 and 6 ml of the above solution to the KDP solution. The above doped solutions were stirred well and then allowed to equilibrate in a dust free zone at room temperature. Small crystals appeared in the beginning stage due to slow evaporation and then grew larger in a considerable time. The grown crystals are represented in the same order as Pure KDP, ZKDP-1, ZKDP-2, ZKDP-3, ZKDP-4 and ZKDP-5.

2.3 Characterization studies

Powder X-ray diffraction (PXRD) studies were carried out on all the grown crystals using an automated X-ray powder diffractometer (X-PERT PRO PANalytical) with monochromated CuK α radiation ($\lambda=1.54056\text{\AA}$). The reflections were indexed by following the procedures of Lipson and Steeple [45]. Lattice parameters along with estimated standard deviation (e.s.d.s) were also determined from the indexed data. Fourier transform infrared (FTIR) spectra were recorded for the Pure KDP and ZKDP-5 crystals by the KBr pellet technique using a Perkin Elmer FTIR spectrometer in the wavenumber range

400 - 4000 cm⁻¹. Atomic absorption spectroscopic (AAS) measurements were carried out for the doped crystals using an AAS spectrometer (model AA-6300). Thermogravimetric analysis (TGA) and differential thermal analysis (DTA) were carried out for the Pure KDP and ZKDP-5 crystals using a thermal analyser (model SDT-Q600) in the nitrogen atmosphere in the temperature range of room temperature to 900° C at a heating rate of 10°C/min. The UV-Vis-NIR spectra were recorded in the wavelength range 190 - 1100nm using a Perkin Elmer Lambda 35 spectrophotometer. The NLO property was tested for all the six grown crystals by carrying out the Kurtz and Perry [46] powder SHG test using a Q-switched Nd:YAG laser (1064nm) (supplied by Spectra Physics, USA). Microhardness measurements were carried out on the (100) face of all the six grown crystals using a SHIMADZU HMV-2T microhardness tester with a diamond indenter.

Crystals with large surface defect-free (i.e. without any pit or crack or scratch on the surface, tested with a travelling microscope) size (>3mm) were selected and used for the AC and DC electrical measurements. The extended portions of the crystal were removed completely and the opposite faces were polished and coated with good quality graphite to obtain a good conductive surface layer. The dimensions of the crystal were measured using a travelling microscope (Least count=0.001cm). The DC electrical conductivity measurements were carried out to an accuracy of ±2% for all the six grown crystals along both a- and c- directions at various temperatures ranging from 40-150°C by the conventional two-probe method using a million megohm meter in a way similar to that followed by Mahadevan and his co-workers [47-49]. The DC conductivity (σ_{dc}) of the crystal was calculated using the relation:

$$\sigma_{dc} = d_{crys} / (RA_{crys})$$

where R is the measured resistance, d_{crys} is the thickness of the sample crystal and A_{crys} is the area of the face of the crystal in contact with the electrode. The capacitance (C_{crys}) and dielectric loss factor ($\tan\delta$) measurements were carried out for all the six grown crystals to an accuracy of ±2% by the parallel plate capacitor method using an LCR meter (Systronics make) with a frequency of 1kHz at various temperatures ranging from 40-150°C along both a- and c- directions in a way similar to that followed by Mahadevan and his co-workers [47-49]. In both the DC and AC electrical measurements, the observations were made while cooling the sample crystal and the temperature was controlled to an accuracy of ±1%. The air capacitance (C_{air}) was also measured but only at 40°C since the temperature variation of C_{air} was found to be negligible. As the crystal surface area touching the electrode was

smaller than the plate (electrode) area of the cell, the dielectric constant of the crystal (ϵ_r) was calculated using Mahadevans's formula [50,51]

$$\epsilon_r = \left\{ \frac{C_{crys} - C_{air} \left(1 - \frac{A_{crys}}{A_{air}} \right)}{C_{air}} \right\} \left(\frac{A_{air}}{A_{crys}} \right)$$

where C_{crys} is the capacitance with crystal (including air), C_{air} is the capacitance of air and A_{air} is the area of the electrode. The AC electrical conductivity (σ_{ac}) was calculated using the relation:

$$\sigma_{ac} = \epsilon_0 \epsilon_r \omega \tan\delta,$$

where ϵ_0 is the permittivity of free space and ω is the angular frequency of the applied field.

III. RESULTS AND DISCUSSION

3.1 Crystal growth, structural analysis and chemical composition

A photograph of the sample crystals grown in the present study is shown in Figure 1. All the grown crystals are stable in atmospheric air, colourless and transparent. Figure 2(a) and 2(b) shows the TGA and DTA curves for the Pure KDP and ZKDP-5 crystals. This study reveals that Pure KDP is thermally stable upto 212°C, after which the sample undergoes an appreciable weight loss. But in ZKDP-5 crystal, the decomposition temperature is shifted to 211°C. There is a slight decrease of temperature for doped crystals, suggesting that substitution of ZnS slightly changes the thermal stability of KDP crystal.



Fig-1: Photograph of the grown crystals

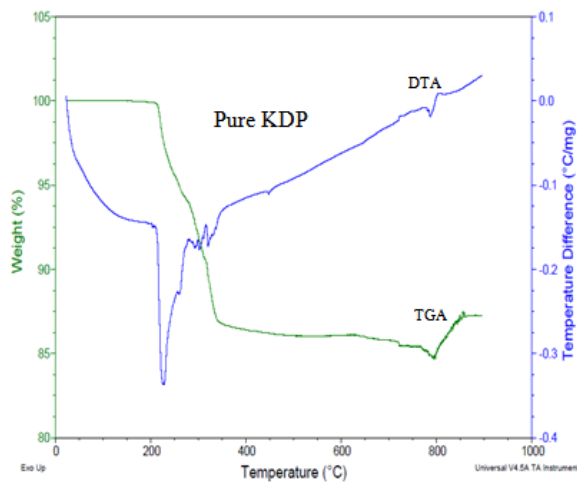


Fig-2(a): TGA and DTA curves observed for the Pure KDP crystal

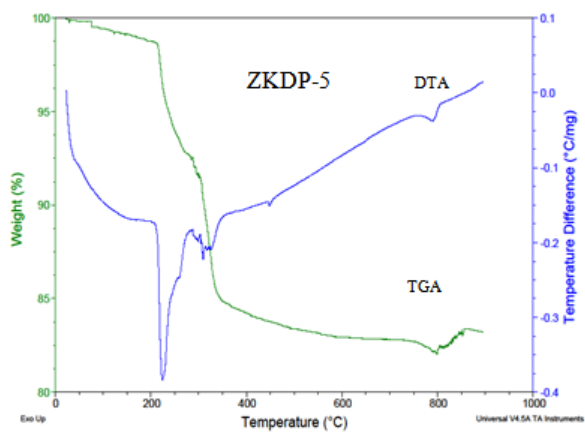


Fig-2(b): TGA and DTA curves observed for ZKDP-5 crystal

The indexed PXRD patterns observed in the present study are shown in Figure 3. In the recorded PXRD pattern, all peaks could be assigned to the tetragonal structure and the appearance of strong and sharp peaks in the PXRD pattern signify the good crystalline and single phase nature of pure and ZnS doped KDP crystals. The average lattice parameters obtained from PXRD data along with the Zn atom contents of doped crystals obtained through the AAS measurements are provided in Table 1. The average lattice parameters observed in the present study (see Table 1) for the Pure KDP crystal agree well with that reported in the literature [52]: This confirms the identity of the substance. The observed increase of lattice volume caused by the impurity addition indicates that the impurity molecules have entered into the KDP crystal matrix. The Zn atom contents observed (see Table 1) endorse this result. So, the present study indicates that it is possible that ZnS can be doped to KDP crystal.

Table-1: Average lattice parameters and Zn atom contents observed

Crystal	Lattice parameters			Zn content (ppm)
	a (Å)	c (Å)	Volume (Å ³)	
Pure KDP	7.413(8)	6.942(9)	381.53	-
ZKDP-1	7.485(5)	7.026(5)	393.68	0.1135
ZKDP-2	7.429(3)	6.962(3)	384.27	0.1528
ZKDP-3	7.510(9)	7.044(6)	397.31	0.1144
ZKDP-4	7.468(6)	6.987(4)	389.64	0.1161
ZKDP-5	7.523(8)	7.063(4)	399.23	0.1659

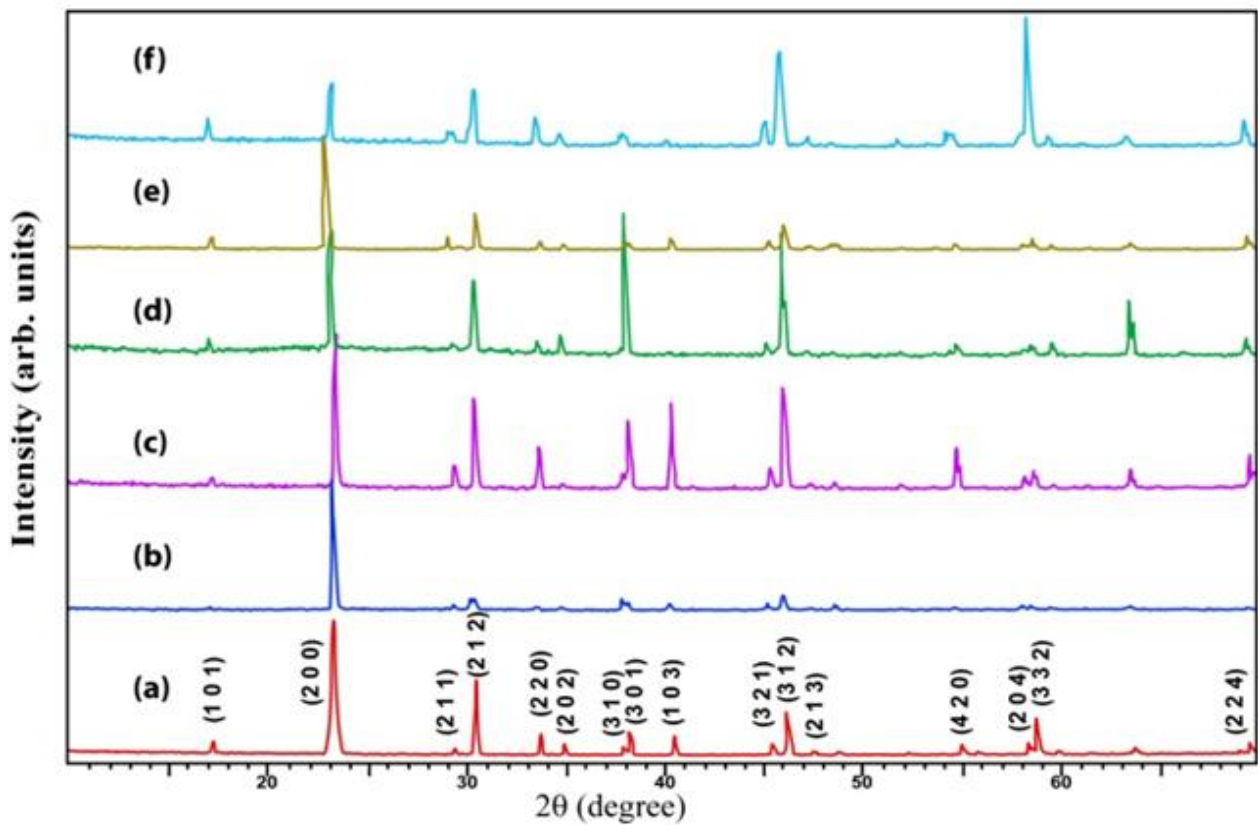


Fig-3: PXRD patterns of (a) Pure KDP, (b) ZKDP-1, (c) ZKDP-2, (d) ZKDP-3, (e) ZKDP-4 and (f) ZKDP-5

Figure 4 shows the FTIR spectra observed for the Pure KDP and ZKDP-5. The vibrational band assignments are provided in Table 2. Significant difference could not be observed for the doped crystals as the impurity concentrations considered are small. The spectrum observed for the Pure KDP compares well with that reported in the literature which again confirms the material of the crystal. The vibrational band assignments reported for Pure KDP in the literature [53] are also given in Table 2 for comparison.

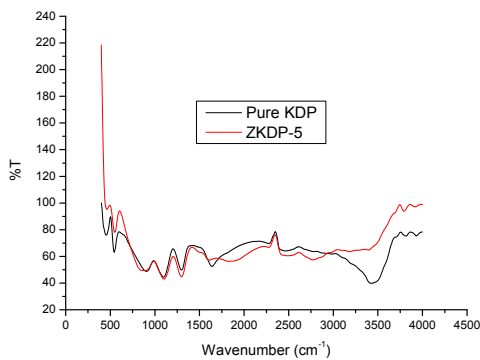


Fig-4: FTIR spectra for the Pure KDP and ZKDP-5 crystals

Table-2: FTIR band assignments

Wavenumbers (cm ⁻¹) for			Assignment
Pure KDP [55]	Pure KDP (Present)	ZKDP-5	
3941	3928	3917	O-H stretching
-	3813	3793	Free O-H stretching
3428	3423	-	Hydrogen bonded O-H stretching
-	-	3185	O-H stretching
2782	-	2775	P-O-H asymmetric stretching
2464	2465	2486	O=P-OH asymmetric stretching
2354	2276	-	P-O-H bending
-	-	1822	O=P-O stretching
1642	1643	1607	O=P-OH symmetric stretching
1300	1298	1298	P=O stretching
1095	1097	1101	P=O stretching
904	906	894	P-O-H stretching
542	544	550	HO-P-OH bending
458	452	462	PO ₄ stretching

3.2 Optical and mechanical properties

The optical transmission range and the transparency cut off limits are important for NLO materials, as it can be put into use only if it possesses the required cut-off wavelength as well as low absorption. The recorded UV-Vis-NIR spectra of pure and ZnS doped KDP crystals are shown in Figure 5. It was observed from the spectra that both pure and ZnS doped KDP crystals have significantly low cut-off wavelengths and good transmittances towards the visible and infrared regions. The percentages of optical transmission and cut-off wavelengths observed for pure and ZnS doped KDP crystals are provided in Table-3. The transparent nature of these crystals observed in the visible region is a desirable property for this material for NLO applications.

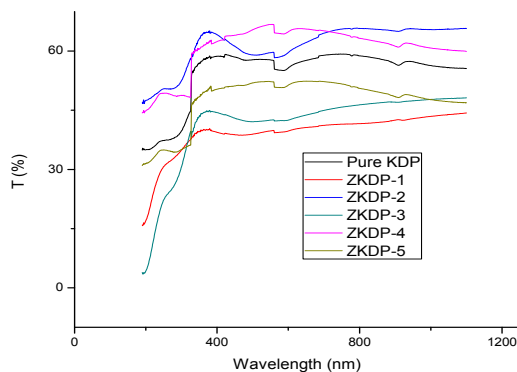


Fig-5: Transmission spectra of pure and ZnS doped KDP single crystals

The SHG efficiency observed for pure and ZnS doped KDP crystals are given in Table 3. It can be observed that SHG efficiency increases due to doping which indicates that all the six crystals grown in the present study are NLO active.

The hardness of a material is a measure of its resistance it offers to local deformations [54]. The micro-indentation test is a useful method for studying the nature of plastic flow and its influence on the deformation of the materials. Higher hardness value of a crystal indicates that greater stress is required to create dislocation [55]. The plots of variation of Vickers hardness number with applied load for pure and ZnS doped KDP single crystals obtained in the present study are shown in Figure 6(a). It can be seen that the hardness value increases with the increase of load for all the six crystals grown. The H_v value increases upto a load of 100g, above which cracks start developing which may be due to the release of internal stress generation with indentation. The Vicker hardness number (H_v) is defined as

$$H_v = 1.8544 P/d^2 \text{ kg/mm}^2$$

and the Meyer's law [52] is expressed as

$$P = k_1 d^n$$

where k_1 is the material constant.

The plots of $\log P$ versus $\log d$ obtained are shown in figure 6(b). The work hardening coefficient or Meyer index (n) was determined from the slop of these plots. The n values obtained are given in Table 3. According to Onitsch and Hanneman ' n ' should lie between 1.0 and 1.6 for hard material and above 1.6 for soft ones [56]. The ' n ' values observed in the present study are more than 1.6. This indicates that all the six crystals grown belong to soft materials category.

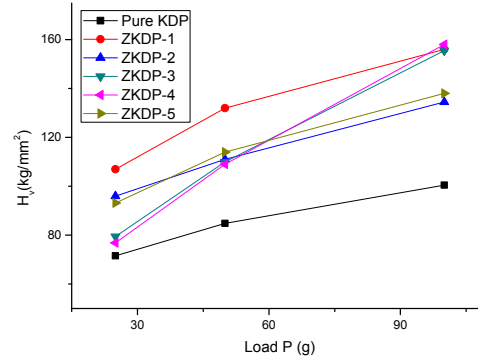


Fig-6(a): Plot of hardness number (H_v) Vs load (P)

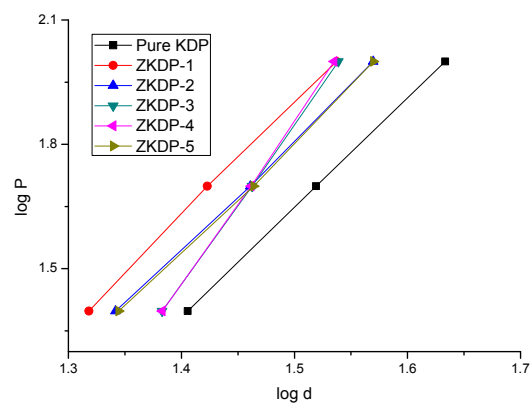


Fig-6(b): Plot of $\log P$ Vs $\log d$

Table-3: The cut off wavelengths, optical transmission percentages, SHG efficiencies and work hardening coefficients (n)

Crystal	Optical transmission (%)	Cut-off wavelength (nm)	SHG efficiency	Work hardening coefficient, n
Pure KDP	58	330	1	2.64
ZKDP-1	45	29	1.863	2.74
ZKDP-2	67	450	1.794	2.64
ZKDP-3	48	250	1.181	3.86
ZKDP-4	65	342	1.969	3.96
ZKDP-5	53	337	1.731	2.67

3.3 Electrical properties

The dielectric parameters, viz. DC electrical conductivity (σ_{dc}), dielectric constant (ϵ_r), dielectric loss factor ($\tan\delta$) and AC conductivity (σ_{ac}) values obtained in the present study are shown in Figures 7-10. It can be seen that all the four parameters increase with the increase in temperature. However, no

systematic variation is observed with the impurity concentration (volume of ZnS solution added to the KDP solution used for the growth of single crystals) for all the above electrical parameters in the whole temperature range considered in the present study. This is illustrated in Figure 11-14.

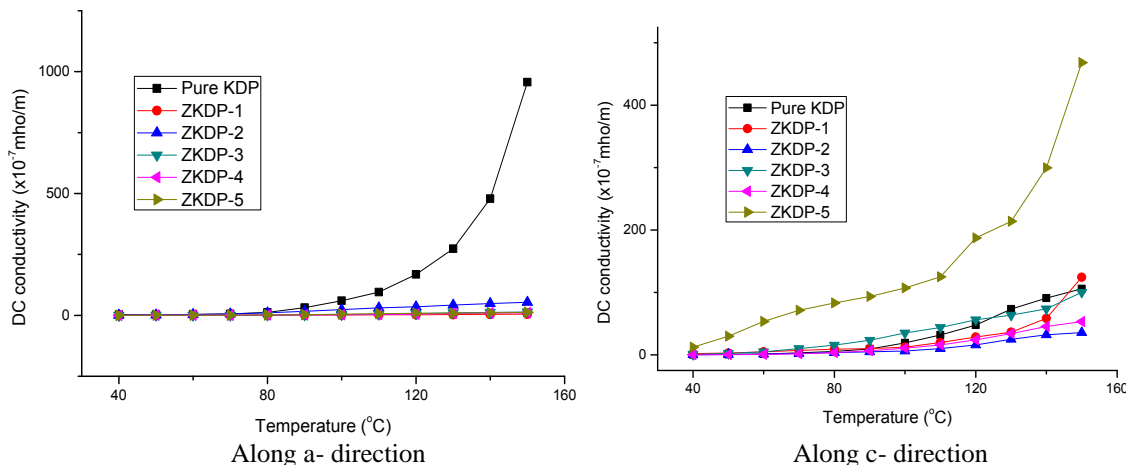


Fig-7: DC electrical conductivities (σ_{dc}) for pure and ZnS doped KDP crystals

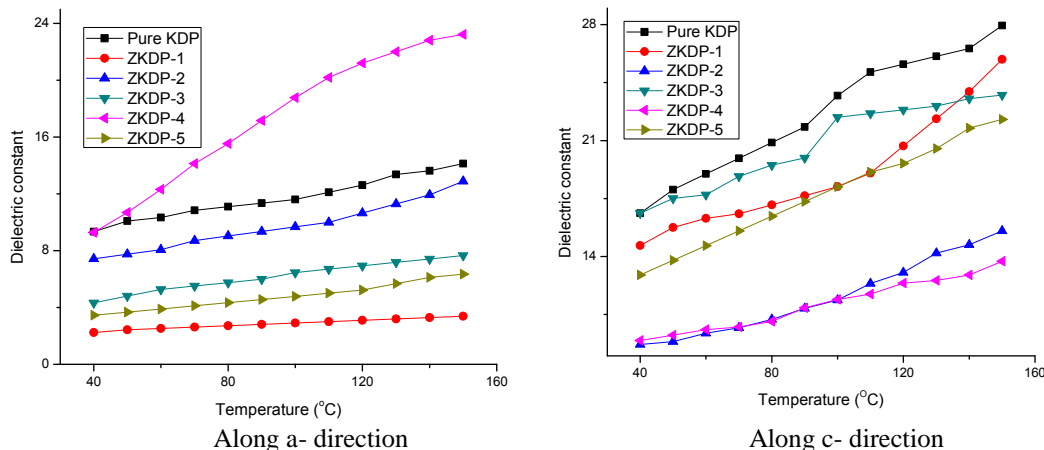


Fig-8: Dielectric constants (ϵ_r) for pure and ZnS doped KDP crystals

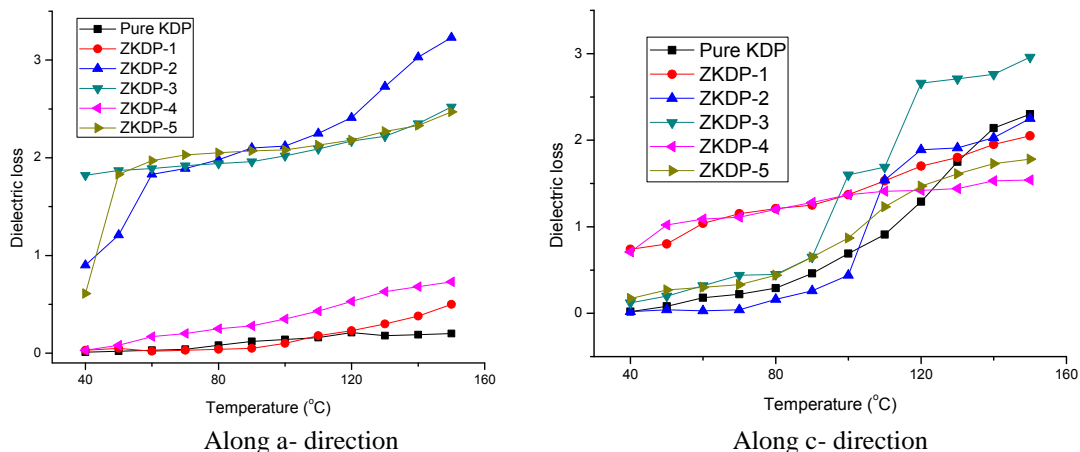
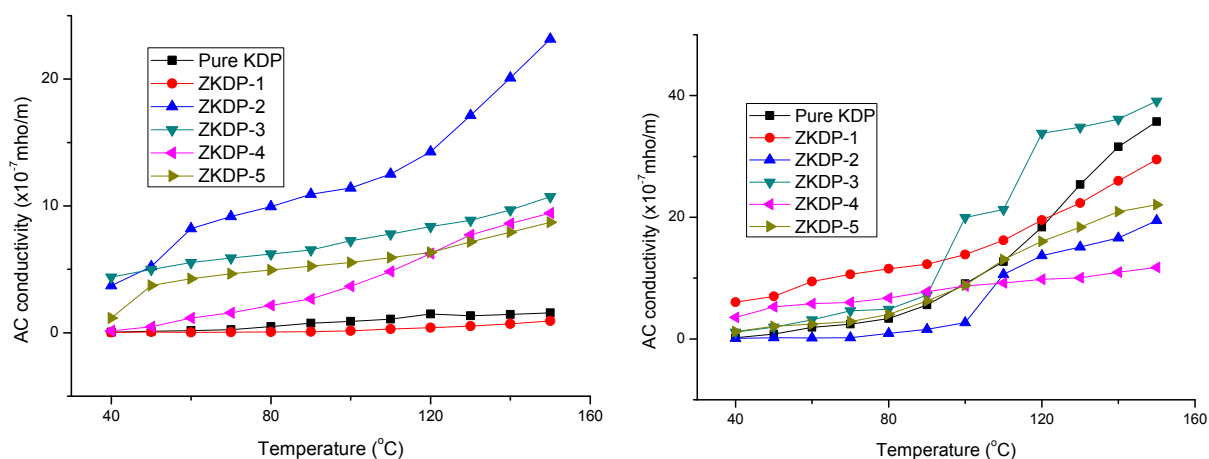


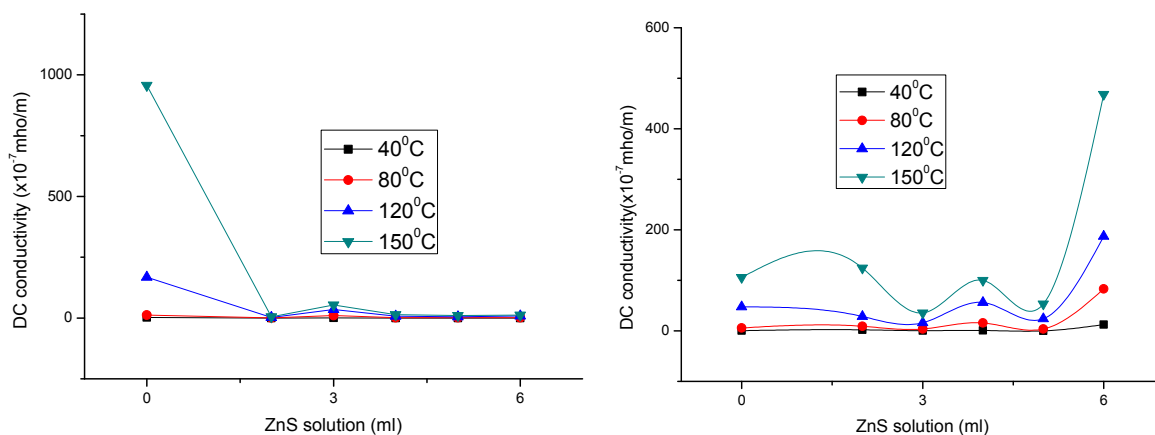
Fig-9: Dielectric loss factors ($\tan\delta$) for pure and ZnS doped KDP crystals



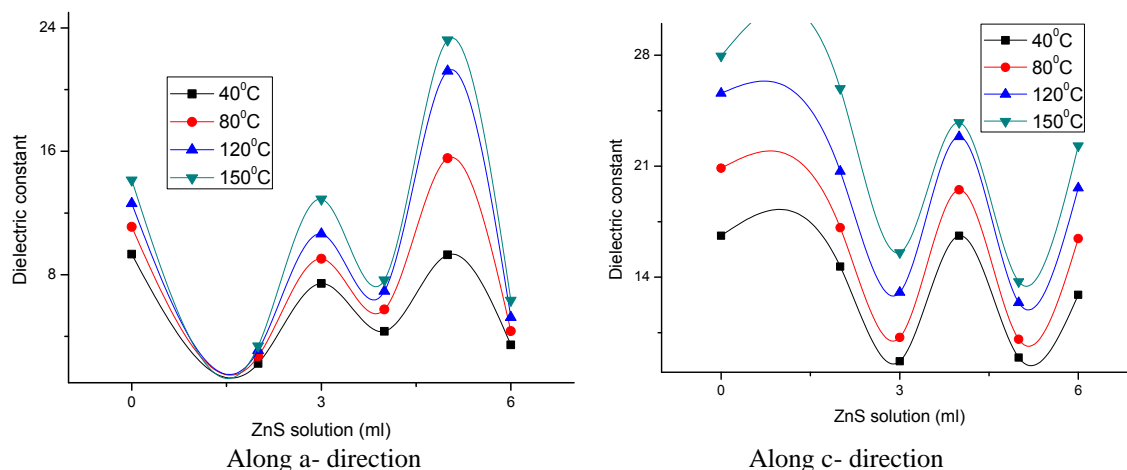
Along a- direction
 Along c- direction
 Fig-10: AC electrical conductivities (σ_{ac}) for the pure and ZnS doped KDP crystals

Moreover, the ϵ_r values (along c- directions) observed for the ZnS doped crystal are less than that observed for the pure KDP. The variation with ZnS

concentration is nonlinear. The decrease of ϵ_r value due to ZnS addition indicates the improvement in NLO property. This is in agreement with the SHG efficiencies observed.



Along a- direction
 Along c- direction
 Fig-11: Impurity concentration dependence of σ_{dc} observed for the pure and ZnS doped KDP crystals



Along a- direction
 Along c- direction
 Fig-12: Impurity concentration dependence of ϵ_r observed for the pure and ZnS doped KDP crystals

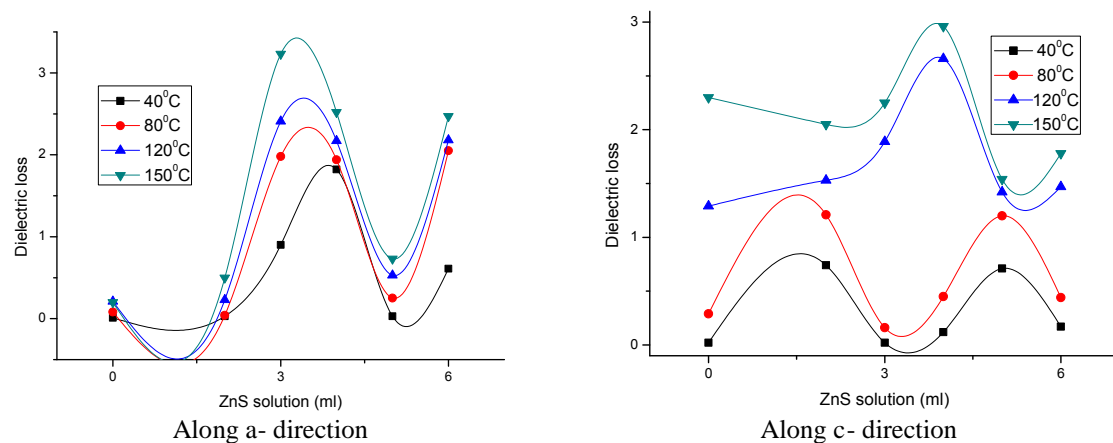


Fig-13: Impurity concentration dependence of $\tan\delta$ observed for the pure and ZnS doped KDP crystals

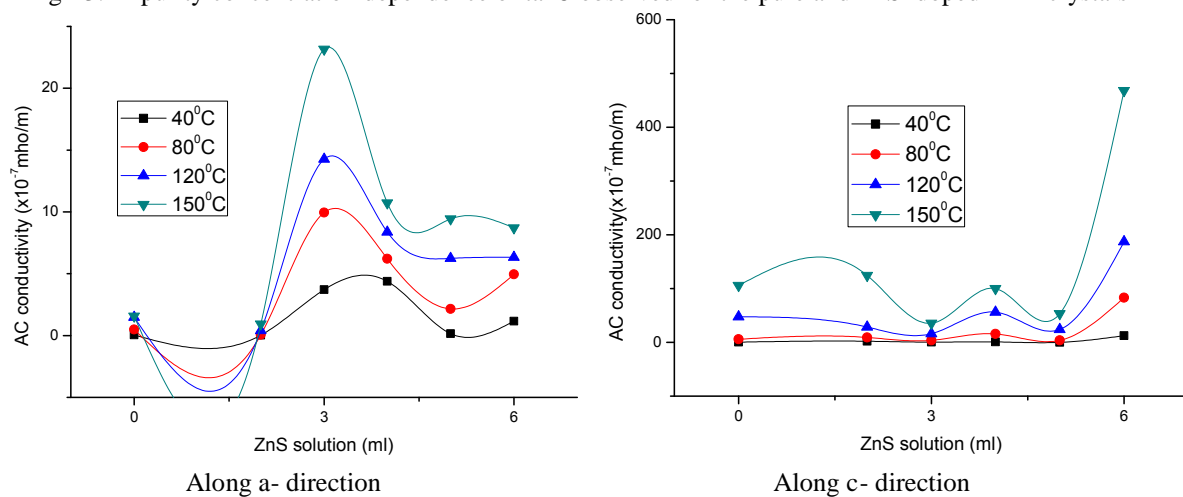


Fig-14: Impurity concentration dependence of σ_{ac} observed for the pure and ZnS doped KDP crystals

The experimental data and especially the character of the temperature dependence of electrical conductivity allowed the earlier workers to understand that the electrical conductivity of KDP crystals is determined by both the thermally generated L-defects (vacant hydrogen bonds) and the foreign impurities incorporated into the lattice and generating L-defects there [57]. When performing measurements, Lokshin [58] assumed that HPO_4^{2-} ions are also responsible for the formation of vacant hydrogen bonds (L-defects). Therefore, the pH value of the initial solution, which determines its ionic composition, can be one of the most important factors that affects crystal conductivity, because of the HPO_4^{2-} ion concentration in the solution at some pH is higher by several orders of magnitude than the concentration of any other impurity [59]. From the above, it can be understood that the proton transport depends on the generation of L-defects. Hence, the increase of conductivity with the increase in temperature observed for ZnS doped KDP crystals in the present study can be understood as due to the temperature dependence of the proton transport.

Also, the conductivity increases smoothly through the temperature range considered in the present study.

Plots between $\ln\sigma_{dc}$ and $10^3/T$ and between $\ln\sigma_{ac}$ and $10^3/T$ (not shown here) are found to be nearly linear. So, the conductivity (DC and AC) values were fitted correspondingly to the Arrhenius relation:

$$\sigma_{dc} = \sigma_{0dc} \exp[-E_{dc}/(kT)]$$

$$\text{and } \sigma_{ac} = \sigma_{0ac} \exp[-E_{ac}/(kT)],$$

where σ_{0dc} and σ_{0ac} are the proportionality constants (considered to be the characteristic constants of the material), k is the Boltzmann constant and T is the absolute temperature. The DC and AC activation energies (E_{dc} and E_{ac}) were estimated using the slopes of the corresponding line plots. The estimated DC and AC activation energies for the pure and ZnS doped KDP crystals grown in the present study are given in Table 4. The E_{dc} values are observed to be more than the E_{ac} values as expected. The low values of E_{dc} and E_{ac} observed suggests that oxygen vacancies may be responsible for conduction in the temperature region considered in the present study.

Variation of dielectric constant with temperature is generally attributed to the crystal expansion, the electronic and ionic polarizations and the presence of impurities and crystal defects. The variation of ϵ_r at lower temperatures is mainly due to the crystal expansion and electronic and ionic polarizations. The increase of ϵ_r at higher temperatures is mainly attributed to the thermally generated charge carriers and impurity dipoles. It has been shown by Varotsos [60] that the electronic polarizability practically remains constant in the case of ionic crystals. So, the increase in dielectric constant with temperature is essentially due to the temperature variation of ionic polarizability.

The ZnS is an ionic substance and is expected to become Zn^{2+} and S^{2-} ions in the solution. In the KDP crystal matrix, some of these ions are expected to occupy interstitial positions. This induces bulk defect states due to competition in getting the sites for the impurity ions to occupy. To some extent, the impurity ions are expected to replace the ions in KDP. So, it is expected to create a random disturbance in the hydrogen bonding system in the KDP crystal matrix. As the conduction in KDP crystal is protonic, the random disturbance in the hydrogen bonding system may cause the electrical parameters to vary nonlinearly with the impurity concentration.

Table-4: The activation energies (E_{ac} and E_{dc}) estimated for pure and ZnS doped KDP crystals

Crystal	Activation energies (eV)			
	Along a- axis		Along c- axis	
	E_{ac} (eV)	E_{dc} (eV)	E_{ac} (eV)	E_{dc} (eV)
Pure KDP	0.148	0.275	0.209	0.260
ZKDP-1	0.153	0.213	0.066	0.159
ZKDP-2	0.068	0.196	0.209	0.266
ZKDP-3	0.036	0.237	0.164	0.198
ZKDP-4	0.161	0.230	0.046	0.314
ZKDP-5	0.059	0.238	0.128	0.133

IV. CONCLUSIONS

ZnS nanoparticles were prepared using ethylene diamine as a capping agent by a simple solvothermal method using a domestic microwave oven. As ZnS nanoparticles prepared were found to be slightly soluble in water (0.71g/100ml of water), ZnS doped KDP single crystals could be successfully grown by the free evaporation method from aqueous solutions at room temperature. The six grown crystals were characterized structurally, chemically, thermally, optically, mechanically and electrically. Results obtained indicate that the impurity molecules have entered into the KDP crystal matrix. ZnS doping

has been found to enhance the SHG efficiency and tune the optical and electrical properties significantly.

REFERENCES

- [1] R.J.Nelmes, G.M.Meyer and J.E.Tibballs, *J.Phys. C Solid State Phys.*,15, 1982, 59.
- [2] T.H.Freeda and C.K.Mahadevan, *Bull.Mater.Sci.*, 23, 2000, 335.
- [3] E.Subbaro, *Ferroelectrics*, 5, 1973, 267.
- [4] D.J.Bae, T.Y.Koo, K.B.Lee, Y.H.Jeung, S.M.Lee and S.I.Kwun, *Ferroelectrics*, 159, 1994, 91.
- [5] M.Rifani, Y.Y.Yin and D.S.Elliott, *J. Am. Chem. Soc.*, 117, 1995, 1512.
- [6] J.B.Beedict, P.M.Wallace and P.J.Reid, *Advanced Materials*, 15, 2003, 1068.
- [7] S.S.Hussaini, N.R.Dhumane, V.G.Dongre, P.Ghughare and M.D.Shirsat, *Optoelectronics and Advanced Materials*, 112, 2007, 707.
- [8] B.Suresh Kumar and Rajendra Badu, *Indian Journal of Pure and Applied Physics*, 46, 2008, 123.
- [9] K.D.Parikh, D.J.Dava, B.B.Parekh and M.J.Joshi, *Cryst.Res.Technol.*, 45(6), 2010, 603
- [10] Ferdousi Akhtar and Jiban Podder, *Journal of Crystallization Process and Technology*, 3, 2011, 55.
- [11] P.Jagadish and N.P.Rajesh, *J. Optoelect. and Adv. Mater.*, 13, 2011, 962.
- [12] G.G.Muley, *Journal of Science and Technology*, 2(5), 2012, 109.
- [13] N.Kanagathara and G.Anbalagan, *International Journal of Optics*, 2012, 2012, 826763.
- [14] G.Bhagavannarayanna, S.Parthiban and S.Meenakshi Sundaran, *Cryst.Growth Des.* 8, 2008, 446.
- [15] P.Kumaresan, S.Moorthy Babu and P.M.Anbarasan, *4th DAE-BRNS Laser Symposium*, 4, 2005, 521.
- [16] L.M.Perez, M.E.Fernandez, J.E.Diosa and R.A.Vargas, *Revista Colomb. De Fisica*, 37, 2005, 86.
- [17] P.Kumarasen, S.Moorthy Babu and P.M.Anbarasan, *Optical Materials*, 30(9), 2001, 1368.
- [18] P.Jagadish and N.P.Rajesh, *J. Optoelect. and Adv. Mater.*,13, 2011, 962.
- [19] E.B.Rudneva, V.L.Manomenova and A.E.Voloshin, *Cryst.Reports*, 51, 2006, 142.
- [20] I.Pritula, V.Gayvoronsky, M.Kopylovsky, M.Kolybaeva, V.Puzikov, A.Kosinova, T.Tkachenko, V.Tsurikov, T.Konstantiniva and V.Pugibko, *J. Funct. Mater*, 15, 2008, 420.

- [21] Valentin G.Grachev, Lan.A.Vrable, Galina, I.Malovichko, Igor M.Pritula, Olga N.Bezkrovnaya, Anna V. Kosinova, Vasyl O.Yatsyna and Vladimir Ya. Gayvoronsky, *J.Appl.Phys.*, 112, 2012, 014107.
- [22] V.Ya Gayvoronsky, M.A. Kopylovsky, M.S.Brodyn, I.M.Pritula M.I.Kolybaeva and V.M.Puzikov, *Laser Phys.Lett*, 10, 2013, 035401.
- [23] I.Pritula, O.Bezkrovnaya, M.Kolybaeva, A.Kosinova, D.Sofrononov, V.Tkachenko and V.Tsurikov, *Material Chemistry and Physics*, 129, 2011, 777.
- [24] Igor Pritula, Vladimir Gayvoronsky, Maria Kolybaeva, Viacheslav Puzikov, Mykhayl Brodyn, Valentin Tkachenko, Anna Kosinova, Maksim Kopylovsky, Vitaliy Tsurikov and Olga Bezkrovnaya, *Optical Materials*, 33, 2011, 623.
- [25] I.Pritula, A.Kosinova, D.A.Vorontsov, M.I. Kolybaeva, O.N. Bezkrovnaya, V.F.Tkachenko, O.M.Vovk and E.V.Grishina, *Journal of Crystal Growth*, 355, 2012, 26.
- [26] O.Conde, A.G.Rolo, M.J.M.Gomes, Ricolleau and D.J.Barber, *Journal of Crystal Growth*, 247, 2003, 371.
- [27] T.M.Hayes, L.B.Lurio, J.Pant and P.D.Persans, *Solid State Comm.*, 117, 2001, 627.
- [28] P.Maly and T.Miyoshi, *J. Lumin.*, 90, 2000, 129.
- [29] A.Meldrum, C.V.White, L.A.Boatner, I.M.Anderson, R.A.Zuhr, E.Sonder, J.D.Budai and D.O.Anderson *Nucl. Ins.Meth.Phys.Res.*, B148, 1999, 957.
- [30] O.Halimi, B.Boudine, M.Sebais, A.Chellouche, R.Mouras and A.Boudrioua, *Material Science and Engineering*, C23, 2003, 1111.
- [31] B.Boudine, M.Sebais, O.Halimi, R.Mouras, A.Boudrioua and P.Bourson, *Optical Materials*, 25, 2004, 373.
- [32] B.Boudine, M.Sebais, O.Halimi, H.Alliouche, A.Boudrioua, and R.Mouras, *Catalysis Today*, 89, 2004, 293.
- [33] A.Bensouici, J.L.Plaza, E.Diequez, O.Halimi, B.Boudine, S.Addala, L.Guebous and M.Sebais, *J. Lumin.*, 129, 2009, 948.
- [34] A.Bensouici, J.L.Plaza, O.Halimi, B.Boudine, M.Sebais and E.Diequez, *Journal of Optoelectronics and Advanced Materials*, 10(11), 2008, 3051.
- [35] K.Balasubramanian, P.Selvarajan and E.Kumar, *Indian Journal of Science and Technology*, 3(1), 2010, 41.
- [36] J. Mu and Y. Zhang, *Appl. Surf. Sci.*, 252, 2006, 7826.
- [37] R.Mach and G.O.Mullar, *Phys. Status Solidi.*, A69, 1982, 11.
- [38] P.V.Mika and S.Lindroos, *Appl. Surf. Sci.*, 136, 1988, 131.
- [39] Y.Andrew Wang, J.Jack Li, Haiyan Chen and Xiaogang Peng, *J. Am.Chem.Soc.*, 124, 2002, 2293.
- [40] Wenzhou Guo, J.Jack Li, Y.Andrew Wang and Xiaogang Peng, *Chem. Mater.*, 15, 2003, 3125.
- [41] Huixiang Tang, Mi Yan, Hui Zhang, Mingzhe Xia and Deren Yang, *Mater. Lett.*, 59, 2005, 1024.
- [42] R.S.S.Saravanan and C.K.Mahadevan, *J.Alloys and Compounds*, 541, 2012,115.
- [43] S.I.Srikrishna Ramya and C.K.Mahadevan, *Mater.lett.*, 89, 2012,111.
- [44] S.Nagaveena and C.K.Mahadevan, *J.Alloys and Compounds*, 582, 2013, 447.
- [45] H.Lipson and H.Steeple, *Interpretation of X-ray powder diffraction patterns* (Newyork, Mac Milton,1970).
- [46] S.K.Kurtz and T.T.Perry, *Appl. Phys.*, 39, 1968, 3798.
- [47] M.Meena and C.K.Mahadevan, *Cryst.Res.Technol.*, 43, 2008, 116.
- [48] S.Perumal and C.K Mahadevan, *Physica B*, 367, 2005, 172.
- [49] G.Selvarajan and C.K Mahadevan, *J.Mater.Sci.*, 41, 2006, 8218.
- [50] S.Goma, C.M Padma and C.K Mahadevan, *Mater.Lett.*, 60, 2006, 3701.
- [51] N.Manonmani, C.K Mahadevan and V.Umayourbhagan, *Mater. Manuf. Process*, 22, 2007, 388.
- [52] T.H Freeda and C.K.Mahadevan, *Pramana-J. Phys.*, 57, 2001, 829.
- [53] F.Loretta, T.Josephine Rani, P.Selvarajan, S.Perumal and S.Ramalingom, *World J. Sci.Technol.*, 1(3), 2011, 1.
- [54] Reena Ittyachan and P.Sagayaraj, *J. Cryst. Growth*, 249, 2003, 557.
- [55] P.Rajesh and P.Ramasamy, *Physica B*, 404, 2009, 1611.
- [56] S.Karan and S.P.Sen Gupta, *Mater.Sci.Eng.*, A398, 2005, 198.
- [57] L.B.Haris and G.J.Vella, *Journal of Applied Physics*, 37 (11), 1967, 4294.
- [58] E.P.Lokshin, *Crystallogr.Rep.*, 41, 1996. 1070.
- [59] E.P.Lokshin, *Crystallogr.Rep.*, 41, 1996. 1061,
- [60] P.Varotsos, *J.Phys.Lett.*, 39, 1978, L79.